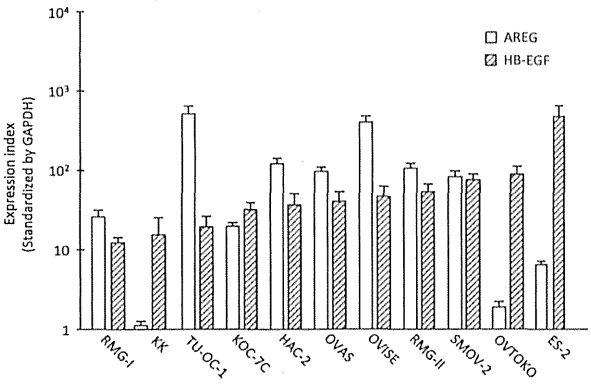

Figure 1. The expression of HB-EGF in 11 ovarian clear cell carcinoma (OCCC) cell lines. The real-time PCR data show the expression of heparin-binding epidermal growth factor-like growth factor (HB-EGF) and amphiregulin (AREG) in OCCC cells. Each value represents the mean (n = 3) and standard deviation (SD) of the mRNA expression index for HB-EGF (diagonal striped bars) and AREG (open bars).

Results

Promotion of HB-EGF expression in response to SN38 treatment

First, we examined the expression of HB-EGF and AREG in 11 cell lines of OCCC. HB-EGF was highly expressed in all of the cell lines, and eight of the 11 cell lines had a high-expression level of AREG (Fig. 1). OVTOKO and ES-2 cells had the highest expression of HB-EGF, while the OVISE and RMG-II cells had higher expression of AREG compared to that of HB-EGF.

To evaluate in vitro anticancer effects of conventional anticancer agents in the OVISE, RMG-II, OVTOKO, and ES-2 cells, cell viability assays were performed using SN38 (Fig. 2A), PTX (Fig. 2B), or CDDP (Fig. 2C). In this analysis, SN38 was a most effective anticancer agent in all four OCCC cell lines. Real-time PCR showed a twofold or higher increase in HB-EGF expression induced by the treatment of the OCCC cells with SN38, and the concentration of HB-EGF also increased more than twofold in the culture medium of RMG-II and ES-2 cells following SN38 treatment (Fig. 3A and B). In contrast, a high concentration of PTX or CDDP did not induce HB-EGF expression in ES-2 cells (Fig. 3C). The addition of the recombinant HB-EGF in cell culture blocked a decrease in cell viability with the treatment of SN38 in OCCC cells (Fig. 3D and E). These results indicated that HB-EGF plays a pivotal role in defense mechanism against the treatment of SN38 in OCCC cells.

To address the potential synergistic anticancer effects of the combination of SN38 and a specific inhibitor of HB-EGF (CRM197), apoptosis assays were performed after treating ES-2 or OVTOKO cells with SN38 and/or CRM197. Treatment with 10 μg/mL of CRM197 and 10 nmol/L of SN38 induced a marked increase in the number of apoptotic ES-2 and OVTOKO cells, compared to

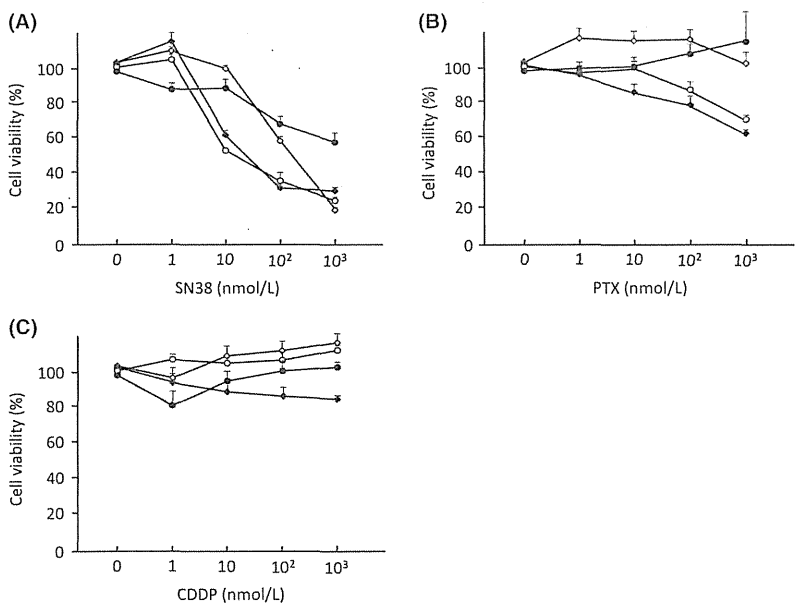

Figure 2. The efficacy of conventional anticancer agents against OCCC cells. Differences in the viability of OVISE (closed squares), RMG-II (closed circles), OVTOKO (open squares), and ES-2 (open circles) OCCC cells after treatment with SN38 (A), paclitaxel (PTX; B), and cisplatin (CDDP; C) for 72 h. Each value represents the mean cell viability rate (n = 3) and the SD. OCCC, ovarian clear cell carcinoma.

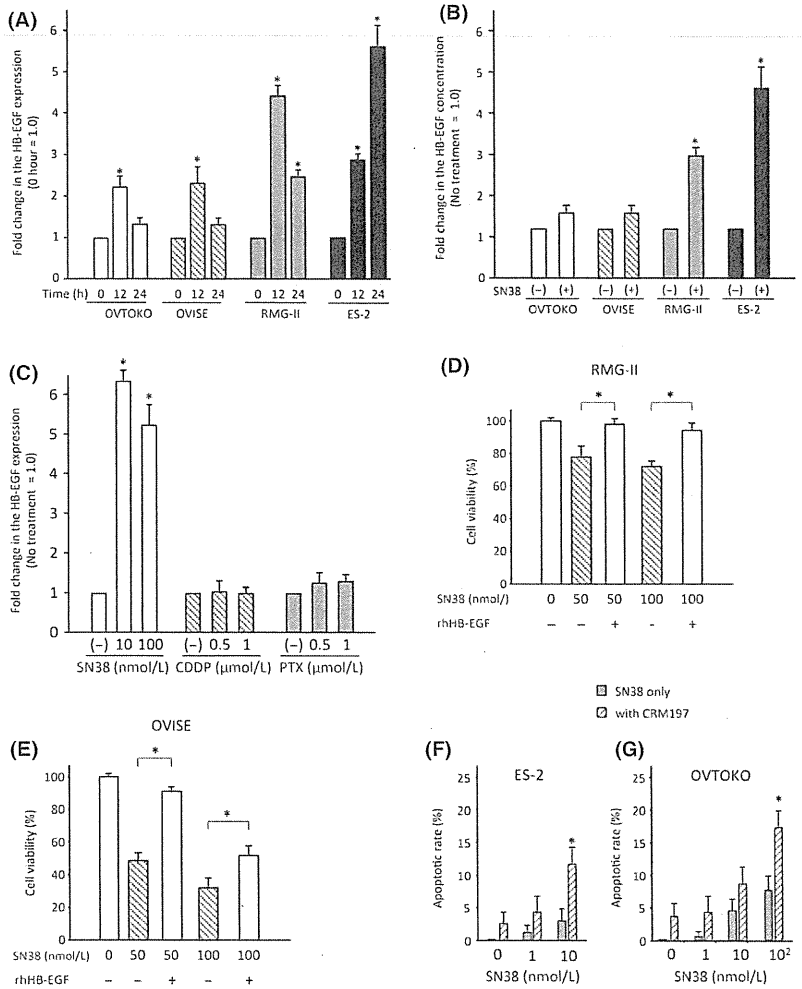

Figure 3. The association between HB-EGF expression and the SN38 treatment of OCCC cells. The induction of HB-EGF mRNA in cells (A) and HB-EGF protein in the culture medium (B) in OVTOKO (open bars), OVISE (diagonal striped bars), RMG-II (gray bars), and ES-2 (closed bars) cells treated with SN38 (10 nmol/L) for 12 or 24 h. Each value represents the mean (n = 3) and SD. (C) The differences in the HB-EGF mRNA expression in ES-2 cells after the treatment with SN38 (open bars), CDDP (diagonal striped bars), or PTX (gray bars). The differences in cell viabilities of RMG-II (D) and OVISE (E), which were cultured with recombinant human HB-EGF (0 and 200 pg/mL) and SN38 (0, 50, and 100 nmol/L). Each value represents the mean fold change (n = 3) and the SD. *P < 0.05. The changes in the apoptosis rate of ES-2 (F) and OVTOKO (G) cells after the treatment with each concentration of SN38 with (closed bars) or without CRM197 (10 μg/mL, diagonal striped bars). Each value represents the mean apoptosis ratio (n = 3) and SD. *P < 0.05, SN38-only versus SN38 with CRM197. HB-EGF, heparin-binding epidermal growth factor-like growth factor; PTX, paclitaxel.

cells with SN38 treatment alone, as determined using TUNEL assay (Fig. 3F and G). These results suggested that the suppression of HB-EGF during the treatment with SN38 leads to a synergistic anticancer effect in OCCC cells.

Screening for transcription factors that regulate the HB-EGF expression induced by SN38 treatment

To identify transcription factor(s) that contribute to the HB-EGF induction following treatment with SN38, a promoter analysis was performed using the ES-2 cells. For the reporter gene analysis, a *HB-EGF* promoter fragment (−2585/+205), which is conserved among mammalian species, fused to a luciferase vector, and various truncated constructs were synthesized. The luciferase assay showed that a reporter vector containing promoter fragment of −178/+205 bp from HB-EGF TSS (pGL/HB$_{-178/+205}$) exhibited an about 20-fold increase in luciferase activity compared to that of pGL/HB$_{-125/+205}$ (Fig. 4A). Additionally, treatment with SN38 induced ~twofold increase in the luciferase activity in a reporter vector containing

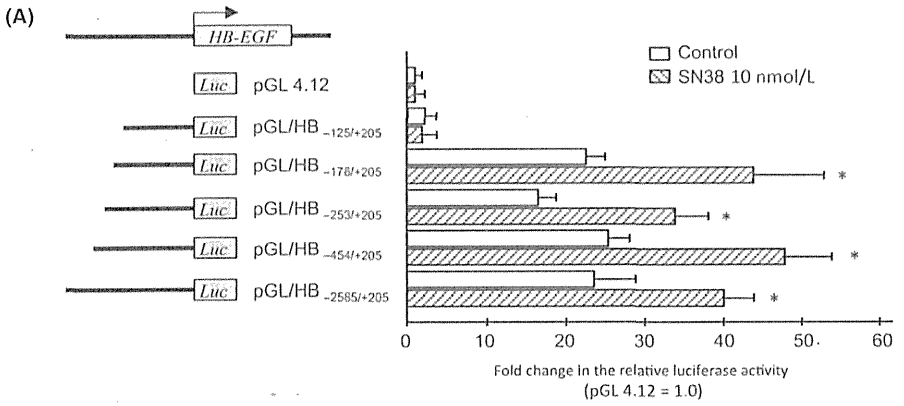

(B)

MatInspector

```
                                    GTGNGCGCBNn ZFP161
                                          nSGGGGCGGGGNnnn SP1
                                          NVKGGGCGGRGYBNn SP1
                                          NNGGGGCGGGGNNnn SP1
                                             GGGCGGGASCn KLF6
                                             nNGSGGGAGGGSGnnnn ZBTB7B
                                               nKGSGAGGGGAGn MAZ
                                                       NVKGGGCGGRGYB SP1
                                                       NNGGGGCGGGGNN SP1
-125 CAGCCCCCGACCCCGCGGGCGCGGCGGAGGACTGGGCGGGAGGAGAGGGCGGCGG-178
       nnnnnHACCCTVBSBGn KLF1
            nBNBGCGCVTGCGCGNB   NRF1
            nnnnnnNVRGGGGYGGSNYCnnn KLF6
                  GGCGYGG   BRE
```

AliBaba 2.1

```
-125 CAGCCCCCGACCCCGCGGGCGCGGCGGAGGACTGGGCGGGAGGAGAGGGCGGCGG -178
          ======SP1=====
                ====WT1===
                ======SP1====
                 ===EGR2===
                      =====SP1===
                         ====GAL4==
                              ======SP1=====
                                   ===TEAD2==
                                     ======SP1=====
                                          =====SP1==
```

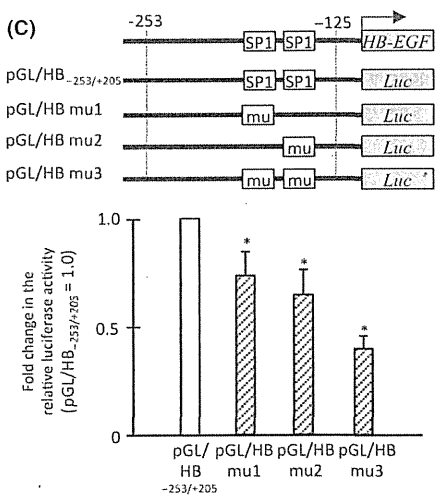

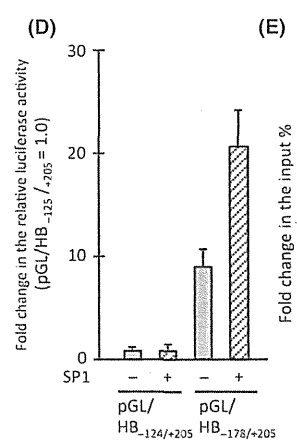

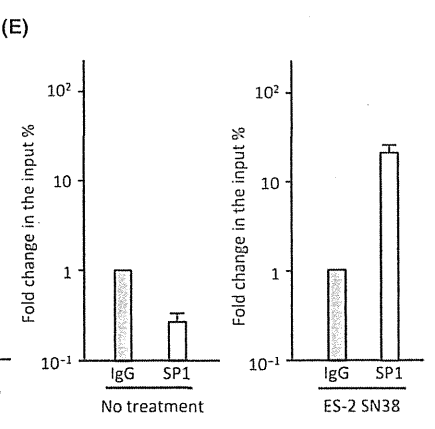

pGL/HB$_{-178/+205}$ compared to the control (Fig. 4A). Accordingly, the sequence located −178 to −125 bp from the TSS of *HB-EGF* was recognized as a promoter sequence bound by transcription factors.

Using the MatInspector (http://www.genomatix.de) and AliBaba 2.1 (http://www.gene-regulation.com) in silico analysis programs, we found that SP1-binding sites are commonly found in this promoter sequence (Fig. 4B). Since the HB-EGF promoter has a TATA-less and GC-rich promoter, which are characteristics of SP1-binding promoters, we focused on SP1 as the candidate transcription factor inducing HB-EGF in SN38-treated ES-2 cells [17, 23, 24].

Reporter vectors with site mutations of each SP1-binding site showed significantly reduced luciferase activity compared to the control (Fig. 4C). Moreover, the luciferase activity significantly decreased, compared to the control, when the two putative binding sites of SP1 were replaced with mutant sites (Fig. 4C). Forced expression of SP1 activated the luciferase activity in 298T cells transfected with pGL/HB$_{-178/+205}$, although no difference was found between the forced expression of SP1 and control in 293T cells transfected by pGL/HB$_{-125/+205}$ (Fig. 4D).

To detect direct interaction between the SP1 protein and HB-EGF promoter in ES-2 cells, a chromatin immunoprecipitation assay was performed in cells with or without treatment with SN38. Quantitative real-time PCR showed that, during treatment with SN38, the level of HB-EGF promoter bound to SP1 significantly increased compared to that of control cells (Fig. 4E). These results indicated that the HB-EGF expression promoted by the treatment with SN38 was regulated by SP1 in OCCC cells.

Contribution of SP1 to the HB-EGF expression and SN38 sensitivity of OCCC cells

To confirm whether SP1 affects the sensitivity of cells to SN38 via the induction of HB-EGF expression, the expression and the cell viability assays were performed after the transfection of small interfering RNA (siRNA) targeting SP1. A Western blot analysis showed that the ES-2 cells transfected with siSP1_1 and siSP1_2 had reduced expression of the SP1 protein compared to the cells transfected with control siRNAs (Fig. 5A). In the ES-2 cells transfected with siSP1_2, the HB-EGF expression was reduced to approximately half the control level, although the HB-EGF expression was not altered in the ES-2 cells transfected with siSP1_1 (Fig. 5B). No induction of HB-EGF expression was found in the presence of SN38 in the ES-2 cells transfected with either siSP1_1 or siSP1_2 (Fig. 5C). Additionally, we examined alterations in the cell viabilities using RMG-II cells, which had the least antitumor effect with the treatment of SN38. Following the treatment with SN38, the number of RMG-II cells transfected with siSP1_1 and siSP1_2 significantly decreased compared to that in the RMG-II cells transfected with control siRNAs (Fig. 6). These results indicate that SP1 regulates the drug sensitivity of SN38 by regulating the HB-EGF expression in OCCC cells.

Discussion

In this study, HB-EGF was attributable for the escape from cell death, as SN38 damaged OCCC cells. SP1 activated HB-EGF expression through its binding to multiple transcription sites within the promoter of HB-EGF in OCCC cells. In addition, the suppression of HB-EGF as well as SP1 enhanced the sensitivity of SN38 in OCCC cells.

SP1, which belongs to the family of SP1/Kruppel-like factor (KFL) transcriptional factors, regulates the expression of numerous genes involved in cell proliferation, apoptosis, and differentiation [25]. Phorbol 12-myristate 13 acetate (PMA) induced an increase in the transcriptional activity of SP1 through the deacetylation of SP1, and also provoked the ectodomain shedding of HB-EGF; it also increased the expression of HB-EGF [26, 27].

Figure 4. The interaction of SP1 with the *HB-EGF* promoter region following SN38 treatment. (A) The alterations in the luminescence of ES-2 cells for each reporter vector in cells with (open bars) and without (diagonal striped bars) SN38 (10 nmol/L) treatment. A schematic diagram showing the reporter vectors on the left side. (B) A schematic diagram obtained from the in silico analysis including the MatInspector and AliBaba 2.1 programs. (C) The luciferase reporter analysis of the site mutants in ES-2 cells. The schematic diagram shows the wild-type SP1-binding sites as "SP1" and the mutated binding sites as "mu" in each vector. The alterations in the luminescence of ES-2 cells among the wild-type reporter vector (open bar) and the mutated reporter vectors (diagonal striped bars) in the presence of SN38 (10 nmol/L). Each value represents the mean (n = 3) and SD. (D) The differences in the relative luciferase activity of 293T cells transfected with pGL/HB$_{-178/+205}$ and the SP1 expression vector (diagonal striped bars). An EGFP expression vector was used as a control (gray bars). Each value represents the mean (n = 3) and SD. All relative luciferase activities were normalized to the renilla luminescence. (E) The results of the ChIP analysis of ES-2 cells with or without SN38 (10 nmol/L) treatment. The fold change in the immunoprecipitated DNA for SP1 (open bars) against templates due to the nonspecific binding with IgG (gray bars). Each value represents the mean (n = 3) and SD. *P < 0.05, versus control. HB-EGF, heparin-binding epidermal growth factor-like growth factor; SP1, specific protein 1.

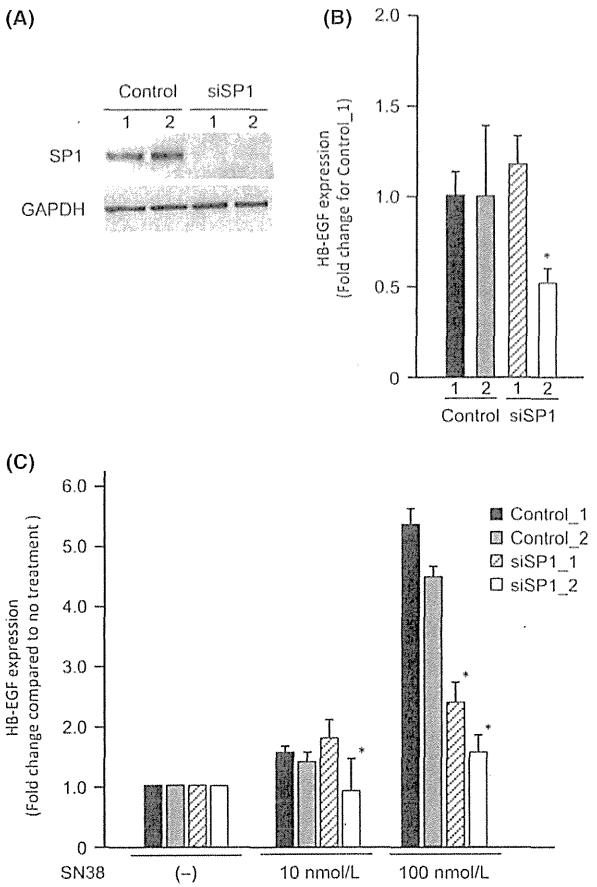

Figure 5. The contribution of SP1 to the HB-EGF induction following the treatment with SN38. (A) A Western blot analysis was performed to confirm the SP1 reduction in the transfected ES-2 cells induced by treatment with siRNAs against SP1 or a control siRNA. (B) The alterations in the HB-EGF mRNA expression in the transfected ES-2 cells induced by treatment with the siRNAs against SP1 or the control siRNA. (C) The induction of HB-EGF mRNA in the RMG-II cells transfected with siRNAs against SP1 or the control siRNA following the treatment of SN38. Each value represents the mean (n = 3) and SD. Closed bars, control_1 siRNA; gray bars, control_2 siRNA; diagonal striped bars, siSP1_1 si RNA; open bars, siSP1_2 siRNA. *P < 0.05, control_1 versus each siRNA. SP1, specific protein 1.

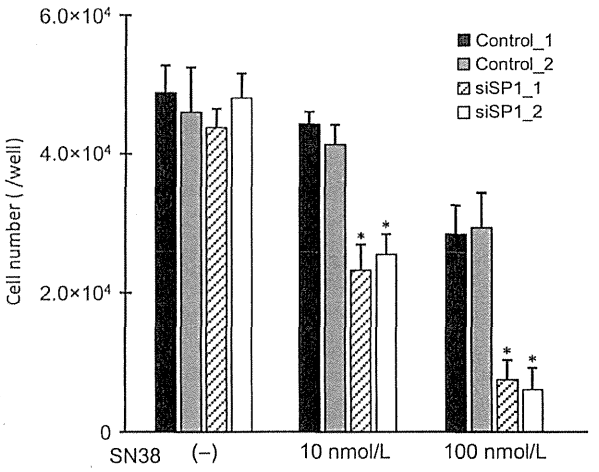

Figure 6. The contribution of SP1 to the cell viabilities following the treatment with SN38. The alterations in the numbers of RMG-II cells transfected with siRNAs against SP1 or a control siRNA after treatment with SN38. Each value represents the mean (n = 3) and SD. Closed bars, control_1 siRNA; gray bars, control_2 siRNA; diagonal striped bars, siSP1_1 si RNA; open bars, siSP1_2 siRNA. *P < 0.05, control_1 versus each siRNA. SP1, specific protein 1.

Additionally, NF-κB induced the expression of HB-EGF, and the NF-κB and SP1 binding sequence was shown to be the same GC-rich element in colon cancer cells [16, 28]. This evidence suggests that SP1 augments the expression of HB-EGF through the deacetylation of SP1 or via an interaction with NF-κB. In mice, SP1 was reported to be directly bound to the promoter regions of HB-EGF [24]. In humans, SP1 also functions as a direct regulator for the expression of HB-EGF, possibly through various posttranslational modifications of SP1 and by interactions with other transcriptional factors.

Dysregulation of SP1 is found in many types of cancer, including ovarian, breast, and gastric cancer, for which HB-EGF is a rational therapeutic target [22, 29, 30]. The hypoxia-inducible factor 2α (HIF2α)–SP1 complex activated coagulation factor VII promoter in OCCC and estrogen receptor α also form complexes with SP1 in other types of ovarian cancer [31, 32]. Additionally, previous reports showed that activation of SP1 promoted breast cancer development and the metastasis of gastric cancer [33, 34]. On the other hand, the SP1 level was highly upregulated in patients with early stage and minimally invasive lung cancer cells and in patients with stage I lung cancer compared to that in lung cancers with high invasiveness and in patients with stage IV lung cancer [35]. These previous findings show that the significance of SP1 involvement in cancer progression have been controversial. In this study, the suppression of SP1 enhanced the sensitivity of OCCC cells to SN38. Therefore, it seems to be important that the suppression of SP1 itself, as well as the inhibition of the posttranslational modifications of SP1, are critical for cancer therapy.

Several compounds that inhibit the transcriptional activity of SP1 have been developed for cancer therapy [25], for example, arsenic trioxide downregulates the expression of SP1 [36]. A phase III trial of arsenic trioxide was performed for patients with acute promyelocytic leukemia classified as having low-to-intermediate risk, and the results suggested that all-*trans*-retinoic acid plus arsenic trioxide may be superior to all-*trans*-retinoic acid

plus other chemotherapy [37]. Bortezomib has been already used for the treatment of patients with multiple myeloma [38, 39]. Bortezomib has been shown to decrease the expression of SP1 and disrupt the interaction of SP1 with NF-κB [40]. Other inhibitory compounds for SP1 will be clinically applied for various diseases, in addition to cancer [41, 42].

We have performed a clinical phase II trial using CRM197 in patients with recurrent and advanced ovarian cancer. To explore the importance of the posttranslational modifications of SP1 in the induction of HB-EGF expression and to search for compounds that can inhibit such modifications, a preclinical study should be performed using combination therapy with CRM197, irinotecan, and a compound that inhibits SP1, such as arsenic trioxide or bortezomib. Such a combination would likely improve the prognosis of patients with OCCC.

Acknowledgments

This work was supported in part by funds from the Central Research Institute of Fukuoka University (Fukuoka, Japan).

Conflict of Interest

None declared.

References

1. Heintz, A. P., F. Odicino, P. Maisonneuve, M. A. Quinn, J. L. Benedet, W. T. Creasman, et al. 2006. Carcinoma of the ovary. FIGO 26th Annual Report on the Results of Treatment in Gynecological Cancer. Int. J. Gynaecol. Obstet. 95(Suppl. 1):S161–S192.
2. del Carmen, M. G., M. Birrer, and J. O. Schorge. 2012. Clear cell carcinoma of the ovary: a review of the literature. Gynecol. Oncol. 126:481–490.
3. Higashiyama, S., J. A. Abraham, J. Miller, J. C. Fiddes, and M. Klagsbrun. 1991. A heparin-binding growth factor secreted by macrophage-like cells that is related to EGF. Science 251:936–939.
4. Higashiyama, S., K. Lau, G. E. Besner, J. A. Abraham, and M. Klagsbrun. 1992. Structure of heparin-binding EGF-like growth factor. Multiple forms, primary structure, and glycosylation of the mature protein. J. Biol. Chem. 267:6205–6212.
5. Elenius, K., S. Paul, G. Allison, J. Sun, and M. Klagsbrun. 1997. Activation of HER4 by heparin-binding EGF-like growth factor stimulates chemotaxis but not proliferation. EMBO J. 16: 1268–1278.
6. Ellis, P. D., K. M. Hadfield, J. C. Pascall, and K. D. Brown. 2001. Heparin-binding epidermal-growth-factor-like growth factor gene expression is induced by scrape-wounding epithelial cell monolayers: involvement of mitogen-activated protein kinase cascades. Biochem. J. 354 (Pt 1):99–106.
7. Murthy, A., V. Defamie, D. S. Smookler, M. A. Di Grappa, K. Horiuchi, M. Federici, et al. 2010. Ectodomain shedding of EGFR ligands and TNFR1 dictates hepatocyte apoptosis during fulminant hepatitis in mice. J. Clin. Invest. 120:2731–2744.
8. Malmsten, M., M. Davoudi, B. Walse, V. Rydengård, M. Pasupuleti, M. Mörgelin, et al. 2007. Antimicrobial peptides derived from growth factors. Growth Factors 25:60–70.
9. Iwamoto, R., S. Yamazaki, M. Asakura, S. Takashima, H. Hasuwa, K. Miyado, et al. 2003. Heparin-binding EGF-like growth factor and ErbB signaling is essential for heart function. Proc. Natl. Acad. Sci. USA 100:3221–3226.
10. Miyamoto, S., M. Hirata, A. Yamazaki, T. Kageyama, H. Hasuwa, H. Mizushima, Y. Tanaka, et al. 2004. Heparin-binding EGF-like growth factor is a promising target for ovarian cancer therapy. Cancer Res. 64: 5720–5727.
11. Yagi, H., S. Miyamoto, Y. Tanaka, K. Sonoda, H. Kobayashi, T. Kishikawa, et al. 2005. Clinical significance of heparin-binding epidermal growth factor-like growth factor in peritoneal fluid of ovarian cancer. Br. J. Cancer 92:1737–1745.
12. Tanaka, Y., S. Miyamoto, S. O. Suzuki, E. Oki, H. Yagi, K. Sonoda, et al. 2005. Clinical significance of heparin-binding epidermal growth factor-like growth factor and a disintegrin and metalloprotease 17 expression in human ovarian cancer. Clin. Cancer Res. 11:4783–4792.
13. Yoshizumi, M., S. Kourembanas, D. H. Temizer, R. P. Cambria, T. Quertermous, and M. E. Lee. 1992. Tumor necrosis factor increases transcription of the heparin-binding epidermal growth factor-like growth factor gene in vascular endothelial cells. J. Biol. Chem. 267:9467–9469.
14. Cheng, C. Y., C. T. Kuo, C. C. Lin, H. L. Hsieh, and C. M. Yang. 2010. IL-1beta induces expression of matrix metalloproteinase-9 and cell migration via a c-Src-dependent, growth factor receptor transactivation in A549 cells. Br. J. Pharmacol. 160:1595–1610.
15. Ornskov, D., E. Nexo, and B. S. Sorensen. 2007. Insulin induces a transcriptional activation of epiregulin, HB-EGF and amphiregulin, by a PI3K-dependent mechanism: identification of a specific insulin-responsive promoter element. Biochem. Biophys. Res. Commun. 354:885–891.
16. Wang, F., R. Liu, S. W. Lee, C. M. Sloss, J. Couget, and J. C. Cusack. 2006. Heparin-binding EGF-like growth factor is an early response gene to chemotherapy and contributes to chemotherapy resistance. Oncogene 26:2006–2016.
17. Kanda, N., and S. Watanabe. 2005. 17 beta-estradiol enhances heparin-binding epidermal growth factor-like

growth factor production in human keratinocytes. Am. J. Physiol. Cell Physiol. 288:C813–C823.
18. Kaneto, H., J. Miyagawa, Y. Kajimoto, K. Yamamoto, H. Watada, Y. Umayahara, et al. 1997. Expression of heparin-binding epidermal growth factor-like growth factor during pancreas development. A potential role of PDX-1 in transcriptional activation. J. Biol. Chem. 272:29137–29143.
19. Chen, X., G. Raab, U. Deutsch, J. Zhang, R. M. Ezzell, and M. Klagsbrun. 1995. Induction of heparin-binding EGF-like growth factor expression during myogenesis. Activation of the gene by MyoD and localization of the transmembrane form of the protein on the myotube surface. J. Biol. Chem. 270:18285–18294.
20. Yanagibashi, T., I. Gorai, T. Nakazawa, E. Miyagi, F. Hirahara, H. Kitamura, et al. 1997. Complexity of expression of the intermediate filaments of six new human ovarian carcinoma cell lines: new expression of cytokeratin 20. Br. J. Cancer 76:829–835.
21. Uchida, T., A. M. Pappenheimer, Jr., and R. Greany. 1973. Diphtheria toxin and related proteins. I. Isolation and properties of mutant proteins serologically related to diphtheria toxin. J. Biol. Chem. 248:3838–3844.
22. Yotsumoto, F., H. Yagi, S. O. Suzuki, E. Oki, H. Tsujioka, T. Hachisuga, et al. 2008. Validation of HB-EGF and amphiregulin as targets for human cancer therapy. Biochem. Biophys. Res. Commun. 365:555–561.
23. Wierstra, I. 2008. SP1: emerging roles—beyond constitutive activation of TATA- less housekeeping genes. Biochem. Biophys. Res. Commun. 372:1–13.
24. Edwards, J. P., X. Zhang, and D. M. Mosser. 2009. The expression of heparin-binding epidermal growth factor-like growth factor by regulatory macrophages. J. Immunol. 182:1929–1939.
25. Chang, W. C., and J. J. Hung. 2012. Functional role of post-translational modifications of Sp1 in tumorigenesis. J. Biomed. Sci. 19:94.
26. Liao, M., Y. Zhang, and M. L. Dufau. 2008. Protein kinase C alpha-induced derepression of the human luteinizing hormone receptor gene transcription through ERK-mediated release of HDAC1/Sin3A repressor complex from Sp1 sites. Mol. Endocrinol. 22:1449–1463.
27. Gechtman, Z., J. L. Alonso, G. Raab, D. E. Ingber, and M. Klagsbrun. 1999. The shedding of membrane-anchored heparin-binding epidermal-like growth factor is regulated by the Raf/mitogen-activated protein kinase cascade and by cell adhesion and spreading. J. Biol. Chem. 274:28828–28835.
28. Xu, J., W. F. Ding, K. K. Shao, X. D. Wang, G. H. Wang, H. Q. Li, et al. 2012. Transcription of promoter from the human APRIL gene regulated by Sp1 and NF-κB. Neoplasma 59:341–347.
29. Miyamoto, S., H. Yagi, F. Yotsumoto, T. Kawarabayashi, and E. Mekada. 2006. Heparin-binding epidermal growth factor-like growth factor as a novel targeting molecule for cancer therapy. Cancer Sci. 97:341–347.
30. Sanui, A., F. Yotsumoto, H. Tsujioka, T. Fukami, S. Horiuchi, K. Shirota, et al. 2010. HB-EGF inhibition in combination with various anticancer agents enhances its antitumor effects in gastric cancer. Anticancer Res. 30:3143–3149.
31. Koizume, S., S. Ito, and E. Miyagi. 2012. HIF2α-Sp1 interaction mediates a deacetylation-dependent FVII-gene activation under hypoxic conditions in ovarian cancer cells. Nucleic Acids Res. 40:5389–5401.
32. Kim, K., R. Barhoumi, R. Burghardt, and S. Safe. 2005. Analysis of estrogen receptor α-Sp1 interactions in breast cancer cells by fluorescence resonance energy transfer. Mol. Endocrinol. 19:843–854.
33. Gorbatenko, A., C. W. Olesen, N. Mørup, G. Thiel, T. Kallunki, E. Valen, et al. 2014. ErbB2 upregulates the Na+, HCO3(−)-cotransporter NBCn1/SLC4A7 in human breast cancer cells via Akt, ERK, Src, and Kruppel-like factor 4. FASEB J. 28:350–363.
34. Zhou, C., J. Ji, Q. Cai, M. Shi, X. Chen, Y. Yu, et al. 2013. MTA2 promotes gastric cancer cells invasion and is transcriptionally regulated by Sp1. Mol. Cancer 12:102. doi: 10.1186/1476-4598-12-102.
35. Hsu, T. I., M. C. Wang, S. Y. Chen, Y. M. Yeh, W. C. Su, W. C. Chang, et al. 2012. Sp1 expression regulates lung tumor progression. Oncogene 31:3973–3988.
36. Jutooru, I., G. Chadalapaka, S. Sreevalsan, P. Lei, R. Barhoumi, R. Burghardt, et al. 2010. Arsenic trioxide downregulates specificity protein (Sp) transcription factors and inhibits bladder cancer cell and tumor growth. Exp. Cell Res. 316:2174–2188.
37. Lo-Coco, F., G. Avvisati, M. Vignetti, C. Thiede, S.M. Orlando, S. Iacobelli, et al. 2013. Retinoic acid and arsenic trioxide for acute promyelocytic leukemia. N. Engl. J. Med. 369:111–121.
38. San Miguel, J. F., R. Schlag, N. K. Khuageva, M. A. Dimopoulos, O. Shpilberg, M. Kropff, et al. 2008. Bortezomib plus melphalan and prednisone for initial treatment of multiple myeloma. N. Engl. J. Med. 359: 906–917.
39. Mateos, M. V., P. G. Richardson, R. Schlag, N. K. Khuageva, M. A. Dimopoulos, O. Shpilberg, et al. 2010. Bortezomib plus melphalan and prednisone compared with melphalan and prednisone in previously untreated multiple myeloma: updated follow-up and impact of subsequent therapy in the phase III VISTA trial. J. Clin. Oncol. 28:2259–2266.
40. Liu, S., Z. Liu, Z. Xie, J. Pang, J. Yu, E. Lehmann, et al. 2008. Bortezomib induces DNA hypomethylation and silenced gene transcription by interfering with Sp1/NF-kappaB-dependent DNA methyltransferase activity in acute myeloid leukemia. Blood 111: 2364–2373.
41. Banerjee, S., D. Kong, Z. Wang, B. Bao, G. G. Hillman, and F. H. Sarkar. 2011. Attenuation of multi-targeted

proliferation-linked signaling by 3,3′-diindolylmethane (DIM): from bench to clinic. Mutat. Res. 728:47–66.
42. Chuengsamarn, S., S. Rattanamongkolgul, B. Phonrat, R. Tungtrongchitr, and S. Jirawatnotai. 2014. Reduction of atherogenic risk in patients with type 2 diabetes by curcuminoid extract: a randomized controlled trial. kJ. Nutr. Biochem. 25:144–150.

Supporting Information

Additional Supporting Information may be found in the online version of this article:

Table S1. Primer sequences.

Table S1. Primer sequences

Primer	Sequence
forward primer for the HB-EGF reporter vector	GCCCATGGTCCCGCACCGAGAGG
reverse primer for pGL/HB$_{-4138/+205}$	GCGGTACCAATGAGAAGGCAGCTGAA
reverse primer for pGL/HB$_{-125/+205}$	GCGGTACCGCTGCCGGCGCCGCGAGCCG
reverse primer for pGL/HB$_{-178/+205}$	GCGGTACCCGCCGCCCTCTCCTCCC
reverse primer for pGL/HB$_{-253/+205}$	GCGGTACCTCCGCCACCTGCCGGTC
forward primer for pGL/HB mu1	aataGCCCGCGGGGTCGGGGGCTG
reverse primer for pGL/HB mu1	CGGAGGACTGGGCGGGAGGAGAGGG
forward primer for pGL/HB mu2	ataCCGCGGGGTCGGGGGCTG
reverse primer for pGL/HB mu2	CGGCGGAGGACTGGGCGGGAGGAGA
forward primer for ChIP PCR	TCCCGTGCTGGGAAGCTCGC
reverse primer for ChIP PCR	TGCCTCGGCCTGGTCCCAAAA

Original Paper

Pathobiology

Pathobiology 2014;81:36–41
DOI: 10.1159/000351721

Received: March 25, 2013
Accepted after revision: April 24, 2013
Published online: August 21, 2013

AKT Activation and Telomerase Reverse Transcriptase Expression are Concurrently Associated with Prognosis of Gastric Cancer

Takamitsu Sasaki[a] Hiroki Kuniyasu[b] Yi Luo[b] Misaho Kitayoshi[b] Eriko Tanabe[b] Daisuke Kato[a] Satoshi Shinya[a] Kiyomu Fujii[b] Hitoshi Ohmori[b] Yuichi Yamashita[a]

[a]Department of Gastroenterolgical Surgery, Fukuoka University School of Medicine, Fukuoka, [b]Department of Molecular Pathology, Nara Medical University, Kashihara, Japan

Key Words
AKT · TERT · Telomerase · Prognosis

Abstract
AKT is a protein in the phosphatidylinositol-3 kinase (PI3K) pathway and associated with diverse pro-tumoral responses. Activation of the human telomere reverse transcriptase (hTERT) is one of AKT's tumorigenic effects. In this study, the significance of AKT phosphorylation and hTERT on prognosis of gastric cancer were examined. AKT activation by epidermal growth factor increased hTERT expression and telomerase activity. In contrast, AKT inactivation by inhibitors and knockdown decreased hTERT expression and telomerase activity in MKN28 gastric cancer cells. In 40 gastric cancer tissues, significant correlations were found among the levels of phosphorylated AKT (pAKT), hTERT expression, and telomer length. The pAKT levels or the levels of pAKT/hTERT were not associated with clinicopathological parameters, including stage and nodal metastasis. However, survival rates of the pAKT-high patients or the pAKT-high and hTERT-high patients were significantly poorer than those in other patients. These findings suggest that AKT and hTERT are good molecular targets for the treatment of gastric cancer.

Introduction

The telomere is a repetitive 'TTAGGG' sequence present at the ends of eukaryotic chromosomes to maintain and protect their integrity [1]. As cells divide, the telomere is shortened in length; thus, the length of the telomere behaves like a marker of the division limit for cells and/or for cell death [2]. In stem cells and cancer cells, the telomere is elongated by telomerase activity, which enables them to divide endlessly [3].

The catalytic subunit of human telomeras reverse transcriptase (hTERT) is responsible for telomerase activity

Abbreviations used in this article

PI3K	Phosphatidylinositol-3 kinase
hTERT	human telomerase reverse transcriptase
pAKT	phosphorylated AKT
EGF	epidermal growth factor
PTEN	phosphatase and tensin homolog deleted on chromosome 10
mTOR	mammalian target of rapamysin
NF	nuclear factor
EMT	epithelial-mesenchymal transition
VEGF	vascular endothelial growth factor

KARGER

E-Mail karger@karger.com
www.karger.com/pat

1015–2008/14/0811–0036$39.50/0

Hiroki Kuniyasu
Department of Molecular Pathology
Nara Medical University
840 Shijo-cho, Kashihara, Nara, 634–8521 (Japan)
E-Mail cooninh@zb4.so-net.ne.jp

and telomere elongation and is suppressed in differentiated cells [4]. In our previous study, we reported that telomere shortening is a significant factor for the induction of TERT expression in gastric mucosa [5].

AKT is a protein in the phosphatidylinositol-3 kinase (PI3K) pathway. Stimulation of receptor tyrosine kinases or G-proteins activates PI3K, which in turn activates AKT. AKT phosphorylation is maintained by heat shock protein 90, and AKT is dephosphorylated by protein phosphatase 2A. Thus, AKT is involved in signaling mediated by various growth factors and cytokines. In particular, insulin-like growth factor-1, epidermal growth factor receptor, and human epidermal growth factor receptor 2, which are important in cancer-progression, activate AKT [6, 7]. Hence, AKT is a one of biomarkers for predicting metastasis of human gastrointestinal cancer [8].

The phosphorylation of AKT modulates signals from phosphatase, tensin homolog deleted on chromosome 10 (PTEN), and the mammalian target of rapamycin to provide diverse effects on cells [9]. In this regard, AKT1 is recognized as an apoptotic inhibitor, which enhances cancer promotion. Phosphorylation via AKT inactivates Bcl-2 antagonist of cell death resulting in its dissociation from Bcl-2. Nuclear factor κB is also activated by AKT, which in turn up-regulates transcription of many survival genes [10]. AKT also induces angiogenesis through the up-regulation of vascular endothelial growth factor (VEGF) [11]. The AKT-microRNA regulatory network suggests that microRNA-mediated gene regulation interacts with the AKT signal pathway [12]. Hence, the expression of AKT is a pivotal tumorigenic factor and AKT is recognized as a relevant molecular target of cancer treatment [7].

The activity of hTERT is regulated by hTERT expression and phosphorylation. Protein kinase C and AKT can phosphorylate hTERT [13, 14]. AKT phosphorylation of hTERT induces intranuclear translocation of hTERT and, subsequently, activates hTERT. In contrast, ring finger protein 1, an E3 ubiquitin ligase, decreases the activity of hTERT by ubiquitylation [15].

In the present study, AKT phosphorylation is correlated with clinicopathological parameters such as TERT expression and telomerase activity in gastric cancer.

Materials and Methods

Cell Culture and Reagents

The human gastric cancer cell line MKN28 (kindly gifted from Professor Wataru Yasui, Hiroshima University, Japan) was maintained in Dulbecco's modified essential medium (Sigma Chemical Co., St. Louis, Mo., USA) containing 10% fetal bovine serum (Sigma Chemical Co.) at 5% CO_2 in air and 37°C. Wortmannin and triciribine were from Biovision LTD. (Milpitas, Calif., USA), and human epidermal growth factor was from Peprotec EC LTD. (Rocky Hill, N.J., USA).

Clinical Materials

Forty gastric tissues (approximately 30 mm^3) were randomly selected from cases diagnosed at the Department of Molecular Pathology, Nara Medical University, between 2001 and 2010. The tissues had been frozen quickly in liquid nitrogen and stored at −80°C. The tissue contents were confirmed by microscopic observation of the adjacent tissues, which were prepared for histopathological examination.

Short Interference RNA

FlexiTube short interference RNAs (siRNAs) for AKT was purchased from Qiagen Genomics, Inc. (Bothell, Wash., USA). All Stars Negative Control siRNA was used as control (Qiagen Genomics, Inc.). Cells were transfected with 50 nM siRNA for each gene using Lipofectamine 2000 (Invitrogen Corp., Carlsbad, Calif., USA) according to the manufacturer's instructions.

Quantitative Reverse Transcription-Polymerase Chain Reaction (qRT-PCR)

Total RNA (1 μg) was used for cDNA synthesis with the ReverTra Ace qPCR RT Kit (Toyobo, Osaka, Japan). qRT-PCR were performed on the StepOne Real-Time PCR System (Applied Biosystems, Foster City, Calif., USA) using the Fast SYBR Green Master Mix (Applied Biosystems) and analyzed by employing the relative standard curve quantification method. The PCR parameters were set according to the manufacturer's instructions and the beta-actin mRNA level was used as internal control. All amplifications were evaluated by melting curve analysis and PCR products were electrophoresed on 2% agarose gels. All PCRs were performed at least in triplicate. Primer sets were purchased from Santa-Cruz.

Immunoblot Analysis

Cell lysates were prepared as described previously [16]. Next, 25 μg (total protein) from lysates were electrophoresed on a 12.5% sodium dodecyl sulfate-polyacrylamide gel followed by electrotransfer to nitrocellulose membranes, which were subjected to immunoblot analysis. The membranes were incubated with primary antibodies and then probed with the appropriate peroxidase-conjugated secondary IgG antibodies (Medical and Biological Laboratories, Nagoya, Japan). Anti-tubulin antibody (LifeSpan Biosciences, Inc., Seattle, Wash., USA), anti-AKT antibody (Rockland Immunochemicals Inc., Gilbertsville, Pa., USA) and anti-phosphorylated AKT antibody (pSer463, Biorbyt, Cambridge, UK) were used as primary antibodies. The immune complex was visualized with the Enhanced Chemiluminescence Western-blot detection system (Amersham, Aylesbury, UK).

Enzyme-Linked Immunosorbent Assay (ELISA)

The lysates prepared as described above were also used for ELISA. Concentrations of pAKT and TERT were evaluated using specific ELISA kits, i.e., Akt (pS473) ELISA kit (Abcam, Cambridge,

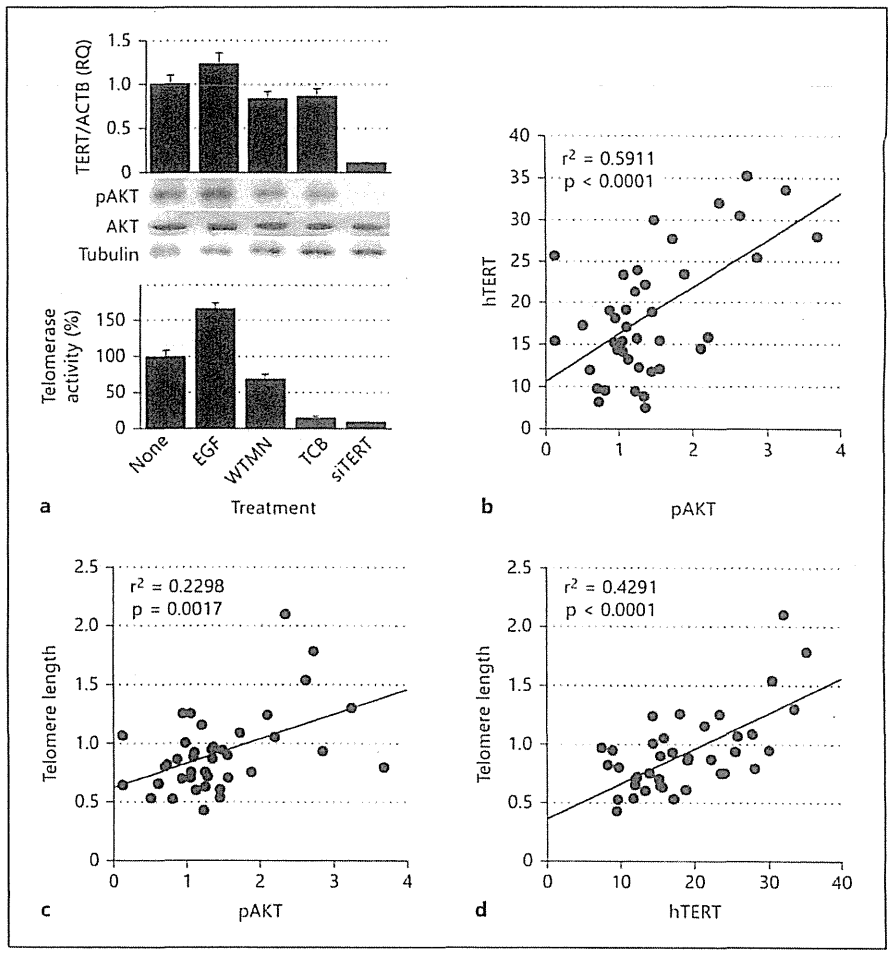

Fig. 1. Relationship between pAKT, hTERT, and telomerase activity. (**a**) Levels of pAKT protein and hTERT mRNA and telomerase activity were compared in MKN28 cells treated with EGF (10 ng/ml), wortmannin (10 nM), triciribine (10 μM), and siRNA against hTERT. Tubulin was used as loading controls. (**b–d**) Levels of pAKT protein and TERT mRNA and telomerase activity were compared in 40 gastric cancer cases. Levels of telomere length, pAKT and hTERT were represented as a relative value to that in peripheral blood lymphocytes, which was set to 1.0.

UK) and human telomerase reverse transcriptase (HTERT) ELISA kit (Oxford Expression Technology, Oxford, UK), according to the manufacturers' instructions.

Telomerase Activity and Telomere Length

Telomerase activity was examined by using the Quantitative Telomerase Detection Kit (US Biomax Inc., Rockville, Md., USA). The telomere length was examined by employing the TeloTAGGG Telomere Length Assay (Roche Applied Science, Indianapolis, Ind., USA). These kits were used according to the manufacturers' instructions.

Statistical Analysis

Statistical analyses of experimental data were carried out using the Spearman r test and ANOVA. The positivities of pAKT and TERT were compared using the two-tailed chi-squared test (InStat, Graphpad Software Inc., La Jolla, Calif., USA). Survival analysis was performed by using the Kaplan-Meier method along with the Logrank test. Univariate and multivariate analyses were calculated by using Cox's hazard model (SPSS Statistics, IBM Japan, Tokyo, Japan). Statistical significance was defined as a two-sided p value of less than 0.05.

Results

To examine the effect of AKT phosphorylation on hTERT expression and telomerase activity, MKN28 gastric cancer cells were analyzed after treatment under different conditions (fig. 1a). Epidermal growth factor stimulated AKT phosphorylation and increased hTERT expression and telomerase activity. In contrast, wortmannin, a PI3K inhibitor, triciribine, an AKT inhibitor, and siRNA-induced AKT knockdown inhibited AKT phosphorylation and decreased hTERT expression and telomerase activity. Total AKT protein levels were not affected by any treatment. These results suggest that AKT phosphorylation is associated closely with hTERT expression and telomerase activity.

Phospho-AKT (pAKT) levels, hTERT protein levels, and telomerase activity were examined in 40 cases of gastric cancer (fig. 1b–d). The pAKT level correlated with the hTERT level and telomerase activity, and the hTERT level correlated with telomerase activity ($p < 0.0001$, $p =$

Table 1. Correlation of pAKT levels with clinicopathological parameters

Parameter	pAKT		p value
	low	high	
Differentiation			
tub1	5	6	
tub2	8	5	
por1	0	2	
por2	5	5	
sig	2	2	NS
Primary tumor			
pT1	4	1	
pT2	3	3	
pT3	6	7	
pT4	7	9	NS
Nodal metastasis			
pN0	7	6	
pN1-2	13	14	NS
Pathological stage			
I	5	3	
II	4	4	
IIIA	6	5	
IIIB	5	3	
IV	0	5	NS
Status			
Survive	13	9	
Dead	7	11	NS

The pathological parameters were evaluated according to Japanese Classification of Gastric Cancer.

Table 2. Correlation of pAKT and hTERT levels with clinicopathological parameters

Parameter	pAKT and hTERT			p value
	both high	intermed	both low	
Differentiation				
tub1	2	8	1	
tub2	2	7	4	
por1	0	2	0	
por2	4	4	2	
sig	1	3	0	NS
Primary tumor				
pT1	1	1	3	
pT2	1	5	0	
pT3	3	8	2	
pT4	4	10	2	NS
Nodal metastasis				
pN0	2	6	5	
pN1-2	7	18	2	NS
Pathological stage				
I	1	4	3	
II	2	5	1	
IIIA	2	7	2	
IIIB	1	6	1	
IV	3	2	0	NS
Status				
Survive	3	14	5	
Dead	6	10	2	NS

The pathological parameters were evaluated according to Japanese Classification of Gastric Cancer.

0.0017, and $p < 0.0001$, respectively). These correlations were compatible to those found in figure 1a.

Next, pAKT levels were compared with clinicopathological parameters (table 1). Parameters in the pAKT-High cases showed no significant difference when compared with those in the pAKT-Low cases. However, survival analysis showed that the pAKT-High cases had a significantly poorer prognosis than pAKT-Low cases (fig. 2a, $p = 0.0498$).

Next, the cases were divided into 3 categories, i.e., pAKT high and TERT high (Both High), pAKT low and TERT low (Both Low), and other cases (Intermediate), to examine the concurrent effect of pAKT and hTERT on disease progression (table 2). As shown in figure 2c, the both high cases were the 9 highest cases of the product of pAKT by hTERT. In contrast, the both low cases were the 7 lowest cases of the product. These cases were distinguishable by distribution of the products. Parameters of the Both-High cases showed no significant differences compared to those of the Both-Low cases. However, the survival analysis showed that the Both-High cases had a significantly poorer prognosis than the Both-Low and Intermediate cases (fig. 2b, $p = 0.0339$), and the Both-Low cases had a significantly better prognosis than the Intermediate cases. Thus, the levels of pAKT and TERT could be useful prognostic markers.

Finally, the significance of pAKT levels or pAKT/hTERT levels was examined by univariate and multivariate analyses to compare stage and nodal metastasis (Table 3). Nodal metastasis emerged as an independent factor for the prognosis, whereas pAKT levels, pAKT/hTERT levels, and stage were dependent factors.

Discussion

In our study, the pAKT level or pAKT/hTERT levels showed no association with any clinicopathological parameters; however, the levels correlated well with disease prognosis.

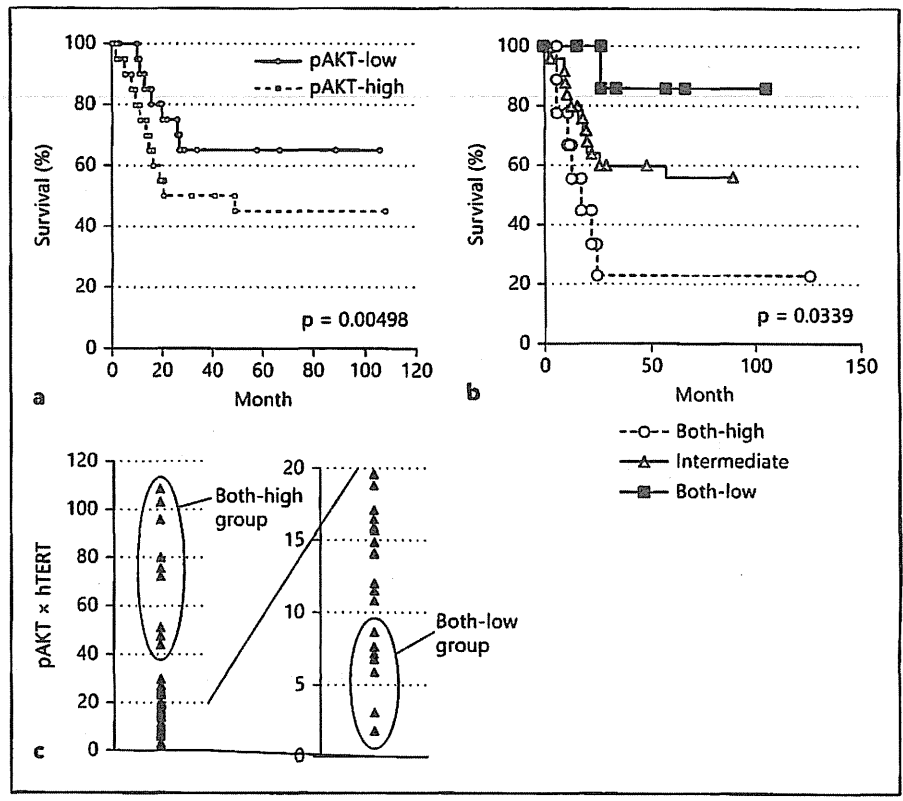

Fig. 2. Survival analyses of 40 gastric cancer cases. (**a**) Overall survival of in 20 cases with higher pAKT levels (pAKT High) was compared with that of 20 cases with lower pAKT levels (pAKT Low) by using the Kaplan-Meier method. (**b**) Overall survivals were compared between 9 cases with high AKT and high TERT (Both High), 7 cases with low pAKT and low TERT (Both High), and 24 cases with intermediate expressions (Intermed) by using the Kaplan-Meier method. (**c**) Distribution of the products of pAKT value by hTERT value in both high group (left panel) and both low group (right panel).

Table 3. Univariate and multivariate analyses of pAKT and/or hTERT levels

	Coefficient	95% CI	p value
Univariate analysis			
Stage	0.0252	0.005–0.524	0.0296
Nodal metastasis	7.613	1.727–33.562	0.0008
pAKT (High, Low)	2.453	0.945–6.368	0.0498
pAKT/hTERT	0.159	0.020–1.243	0.0198
Multivariate analysis			
Stage	1.077	0.236–4.916	0.9351
Nodal metastasis	0.132	0.028–0.627	0.0108
pAKT (high, low)	0.572	0.236–1.389	0.2172
pAKT/hTERT	0.793	0.267–2.353	0.7995

CI = Confidence interval. Both high, both low, intermed.

AKT is associated with cancer cell survival through altering Bcl-2 antagonist of cell death, p53, forkhead, nuclear factor κB, mammalian target of rapamycin, and PTEN [10] [17]. Moreover, dysregulated PTEN/PI3K/AKT signaling interacts with the Wingless-INT pathway to induce epithelial-mesenchymal transition (EMT), which is usually associated with cancer stem cell-phenotype and poor prognosis [18]. It has been recently reported that hTERT promotes transforming growth factor-β and β-catenin-induced EMT by inducing β-catenin nuclear translocation and its transcriptional activity for vimentin expression [19]. Therefore, PTEN/PI3K/AKT signaling enhances EMT and stem cell phenotypes. In the present study, the association of AKT phosphorylation, TERT expression, and telomerase activity was confirmed in MKN28 gastric cancer cells and tissues of 40 gastric cancer patients. These associations could result in poor prognoses in cases with high pAKT levels or high pAKT/hTERT levels. Multivariate analysis revealed that pAKT levels or pAKT/hTERT levels were dependent prognostic factors. The examination of more gastric cancer cases is required to confirm the hypothesis that the EMT/stem cell phenotype affects disease progression.

Angiogenesis is an essential phenotype for cancer progression [20]. VEGF expression is associated closely with neovascularization and cancer progression in many malignancies. The PI3K/AKT pathway is one of the inducers of a VEGF response, which includes other inducers such as mitogen-activated protein kinase (extracellular signal-regulated kinases or p38), Src, focal adhesion kinase, Rho family GTPases, and endothelial nitric oxide [21]. The

PI3K/AKT pathway increases the secretion of VEGF from cancer cells by hypoxia-inducible factor 1-dependent and -independent mechanisms [22]. Therefore, AKT suppression could result in an anti-angiogenic effect on gastric cancer.

Our data showed that AKT and hTERT were widely expressed in gastric cancer. The concurrent expression of these 2 proteins at high levels is associated with a poor prognosis. These results suggest that AKT and hTERT are good molecular targets for the treatment of gastric cancer.

References

1 Blackburn EH: Switching and signaling at the telomere. Cell 2001;106:661–673.
2 Lingner J, Cooper JP, Cech TR: Telomerase and DNA end replication: No longer a lagging strand problem? Science 1995;269:1533–1534.
3 Stewart SA, Weinberg RA: Telomeres: Cancer to human aging. Annu Rev Cell Dev Biol 2006;22:531–557.
4 Autexier C, Lue NF: The structure and function of telomerase reverse transcriptase. Annu Rev Biochem 2006;75:493–517.
5 Kuniyasu H, Kitadai Y, Mieno H, Yasui W: Helicobactor pylori infection is closely associated with telomere reduction in gastric mucosa. Oncology 2003;65:275–282.
6 Sukawa Y, Yamamoto H, Nosho K, Kunimoto H, Suzuki H, Adachi Y, Nakazawa M, Nobuoka T, Kawayama M, Mikami M, Matsuno T, Hasegawa T, Hirata K, Imai K, Shinomura Y: Alterations in the human epidermal growth factor receptor 2-phosphatidylinositol 3-kinase-v-AKT pathway in gastric cancer. World J Gastroenterol 2012;18:6577–6586.
7 Berg M, Soreide K: EGFR and downstream genetic alterations in KRAS/BRAF and PI3K/AKT pathways in colorectal cancer: Implications for targeted therapy. Discov Med 2012;14:207–214.
8 Ng L, Poon RT, Pang R: Biomarkers for predicting future metastasis of human gastrointestinal tumors. Cell Mol Life Sci 2013;in press.
9 Cheung M, Testa JR: Diverse mechanisms of AKT pathway activation in human malignancy. Curr Cancer Drug Targets 2013;13:234–244.
10 Downward J: PI 3-kinase, AKT and cell survival. Semin Cell Dev Biol 2004;15:177–182.
11 Radisavljevic Z: AKT as locus of cancer angiogenic robustness and fragility. J Cell Physiol 2013;228:21–24.
12 Xu M, Mo YY: The AKT-associated microRNAs. Cell Mol Life Sci 2012;69:3601–3612.
13 Li H, Zhao L, Yang Z, Funder JW, Liu JP: Telomerase is controlled by protein kinase Cα in human breast cancer cells. J Biol Chem 1998;273:33436–33442.
14 Kang SS, Kwon T, Kwon DY, Do SI: Akt protein kinase enhances human telomerase activity through phosphorylation of telomerase reverse transcriptase subunit. J Biol Chem 1999;274:13085–13090.
15 Kim JH, Park SM, Kang MR, Oh SY, Lee TH, Muller MT, Chung IK: Ubiquitin ligase MKRN1 modulates telomere length homeostasis through a proteolysis of hTERT. Genes Dev 2005;19:776–781.
16 Kuniyasu H, Oue N, Wakikawa A, Shigeishi H, Matsutani N, Kuraoka K, Ito R, Yokozaki H, Yasui W: Expression of receptors for advanced glycation end-products (RAGE) is closely associated with the invasive and metastatic activity of gastric cancer. J Pathol 2002;196:163–170.
17 Populo H, Lopes JM, Soares P: The mTOR signalling pathway in human cancer. Int J Mol Sci 2012;13:1886–1918.
18 Karamitopoulou E: Tumor budding cells, cancer stem cells and epithelial-mesenchymal transition-type cells in pancreatic cancer. Front Oncol 2012;2:209.
19 Liu Z, Li Q, Li K, Chen L, Li W, Hou M, Liu T, Yang J, Lindvall C, Bjorkholm M, Jia J, Xu D: Telomerase reverse transcriptase promotes epithelial-mesenchymal transition and stem cell-like traits in cancer cells. Oncogene 2012;advance online publication.
20 Fidler IJ: The pathogenesis of cancer metastasis: The 'seed and soil' hypothesis revisited. 2003;3:453–458.
21 Claesson-Welsh L, Welsh M: VEGFA and tumour angiogenesis. J Intern Med 2013;273:114–127.
22 Karar J, Maity A: PI3K/AKT/mTOR pathway in angiogenesis. Front Mol Neurosci 2011;4:51.
23 Japanese Gastric Cancer Association: Japanese classification of gastric carcinoma: 3rd English edition. Gastric Cancer 2011;14:101–112.

MOLECULAR AND CLINICAL ONCOLOGY 2: 751-755

Expression of human epidermal growth factor receptor 2 in primary and paired parenchymal recurrent and/or metastatic sites of gastric cancer

RYOSUKE SHIBATA[1], SATOSHI NIMURA[2], TATSUYA HASHIMOTO[1], TORU MIYAKE[1], SHINSUKE TAKENO[1], SEIICHIRO HOSHINO[1], KAZUKI NABESHIMA[2] and YUICHI YAMASHITA[1]

Departments of [1]Gastroenterological Surgery and [2]Pathology, Fukuoka University Faculty of Medicine, Fukuoka 814-0180, Japan

Received May 13, 2014; Accepted June 10, 2014

DOI: 10.3892/mco.2014.329

Abstract. Human epidermal growth factor receptor 2 (HER2) status has been evaluated at the primary site of gastric cancer when planning trastuzumab therapy against recurrent or metastatic lesions, since tissue sampling is uncommon in recurrent or metastatic lesions. This study retrospectively investigated the concordance of HER2 expression between primary and metastatic/recurrent lesions in order to confirm sensitivity to trastuzumab. The subjects comprised 37 patients with gastric adenocarcinoma who underwent tissue biopsy or surgical resection of the primary sites and 49 paired synchronous or metachronous metastatic sites (excluding lymph nodes) at the Fukuoka University Hospital between January, 1998 and September, 2012. All the samples were evaluated for HER2 status at the invasive front by immunohistochemistry (IHC). The HER2 positivity rate of the primary sites was ~16% and the concordance ratio of the IHC results between primary and paired metastatic sites was ~97%. No discordant cases regarding HER2 status were found among metachronous interventions for metastatic lesions. Only one patient exhibited conversion from a HER2-negative status in all the portions of the primary site to a positive status in a metastatic site. In conclusion, a high concordance ratio for HER2 status was observed between primary and paired metastatic lesions. Thus, employing trastuzumab therapy against metastatic or recurrent gastric cancer based on the HER2 status of the primary lesion appears to be an acceptable approach.

Correspondence to: Dr Ryosuke Shibata, Department of Gastroenterological Surgery, Fukuoka University Faculty of Medicine, Nanakuma 7-45-1, Jonan-ku, Fukuoka 814-0180, Japan
E-mail: ryosukeshibata@hotmail.com

Key words: human epidermal growth factor receptor 2, concordance, multiple intervention, inoperable gastric cancer

Introduction

Gastric cancer is one of the most commonly diagnosed cancers and the second most common cause of cancer-related mortality worldwide (1,2). Radical gastrectomy and lymph node dissection with adjuvant chemotherapy are performed for patients with advanced gastric cancer (3). However, metastatic gastric cancer has a 5-year survival rate of 5-20% and a median overall survival of <1 year (1,4,5). In 2010, trastuzumab combined with chemotherapy was established as a new standard treatment option for human epidermal growth factor receptor 2 (HER2)-positive advanced gastric or gastroesophageal junction cancer by the ToGA study (6). Although trastuzumab combination therapy is adopted for inoperable advanced or metastatic disease, the HER2 status is commonly evaluated in the primary lesion, since metastatic sites are rarely resected or biopsied prior to treatment. With breast cancer, however, the concordance ratio for HER2 status between the primary lesion and metastatic lymph nodes was reported to be 90-98% (7,8), whereas the concordance ratio for HER2 status between primary and metastatic sites other than lymph nodes was reported to be lower (9,10). However, although a high concordance ratio for HER2 status between primary and lymph node lesions has been reported in gastric cancer (11,12), a concordance ratio for HER2 status between primary and metastatic lesions other than lymph nodes has not been reported. In addition, HER2 status is typically evaluated by immunohistochemistry (IHC) and/or fluorescence *in situ* hybridization (FISH) and a high concordance ratio between IHC and FISH has been reported (13).

In this study, HER2 expression was assessed using IHC (IHC score 2+) and FISH in the primary lesion and in paired metastatic lesions other than lymph nodes. The aim of this study was to investigate the concordance of HER2 expression between primary and metastatic lesions and the feasibility of using HER2 expression in the primary lesion for determining therapy against metastatic lesions.

Patients and methods

Patients and tissue samples. The samples used in this study were surgically resected or biopsied at Fukuoka University

Table I. Clinicopathological characteristics of the study population.

Characteristics	Total (%)	No. of primary sites (%) (n=37)	No. of metastatic sites (%) (n=49)
Age (years)			
Median	64		
Range	45-80		
Gender			
Male	30 (81.0)		
Female	7 (19.0)		
Type of intervention			
Surgical resection	75 (87.0)	28 (76.0)	47 (96.0)
Biopsy	11 (13.0)	9 (24.0)	2 (4.0)
Histological type			
Differentiated	13 (35.0)		
Undifferentiated	17 (46.0)		
Mixed	7 (19.0)		
Metastasis			
Synchronous	19 (39.0)		
Metachronous	30 (61.0)		
Pre-intervention chemotherapy of metastatic sites			
UFT	9 (18.0)		
S-1	9 (18.0)		
Others	5 (10.0)		
None	24 (54.0)		

UFT, uracil-tegafur; S-1, tegafur-gimeracil-oteracil potassium.

Table II. Human epidermal growth factor receptor 2 (HER2) status of primary and metastatic sites.

	Metastatic sites				
	Negative			Positive	
HER2 status	0	1+	2+ (FISH-)	2+ (FISH+)	3+
Primary sites					
Negative					
0	28	1	0	0	1
1+	1	0	0	0	0
2+ (FISH-)	0	0	0	0	0
Positive					
2+ (FISH+)	0	0	0	0	1
3+	0	0	0	0	5

FISH, fluorescence *in situ* hybridization.

Table III. Association of human epidermal growth factor receptor 2 (HER2) status of the primary site with histological type and type of intervention.

	HER2 status		
Variables	Negative	Positive	P-value
Histological type			0.0244
Differentiated	8	5	
Undifferentiated	16	1	
Mixed	7	0	
Type of intervention			>0.9999
Surgical resection	23	5	
Biopsy	8	1	

Table IV. Concordance of human epidermal growth factor receptor 2 (HER2) status between primary and paired metastatic lesions.

	Metastatic site		
HER2 status	Negative	Positive	P-value
Primary site			<0.0001
Negative	30	1	
Positive	0	6	

Hospital between January, 1998 and September, 2012. A total of 37 patients with gastric adenocarcinoma (9 biopsies and 28 resection specimens) and 49 paired synchronous or metachronous metastatic tissues (2 biopsies and 47 resection specimens) were analyzed. The invasive front of the resected tumor tissues was examined immunohistochemically. None of the patients received neoadjuvant therapy and 23 metastatic tissue samples were obtained from patients who had been treated with chemotherapy. No patients received trastuzumab combination therapy. Metachronous metastasis was defined as metastasis arising >6 months following curative resection.

HER2 expression and amplification. HER2 status was examined using 10% formalin-fixed paraffin-embedded tissues. Immunohistochemical staining was performed automatically with the Ventana iView PATHWAY HER2 (4B5) (Ventana Medical Systems, Roche, Tucson, AZ, USA). Antigen activation was performed in citrate buffer under high pressure. HER2 immunoreactivity was scored as negative (0 or 1+), equivocal (2+) and positive (3+) by an experienced pathologist according to the scoring system described by Hofmann *et al* (14).

The PathVysion HER2 DNA Probe kit (Abbott Molecular, Abbott Park, IL, USA) and a BioView Duet-3 scanning system (BioView, Ltd., Rehovot, Israel) with fluorescence microscopy (BX51 TRF; Olympus, Nagano, Japan) were used for FISH. Gene amplification was scored when a minimum of 20 cancer cell nuclei exhibited a HER2/chromosome enumeration probe (CEP)17 ratio of >2.

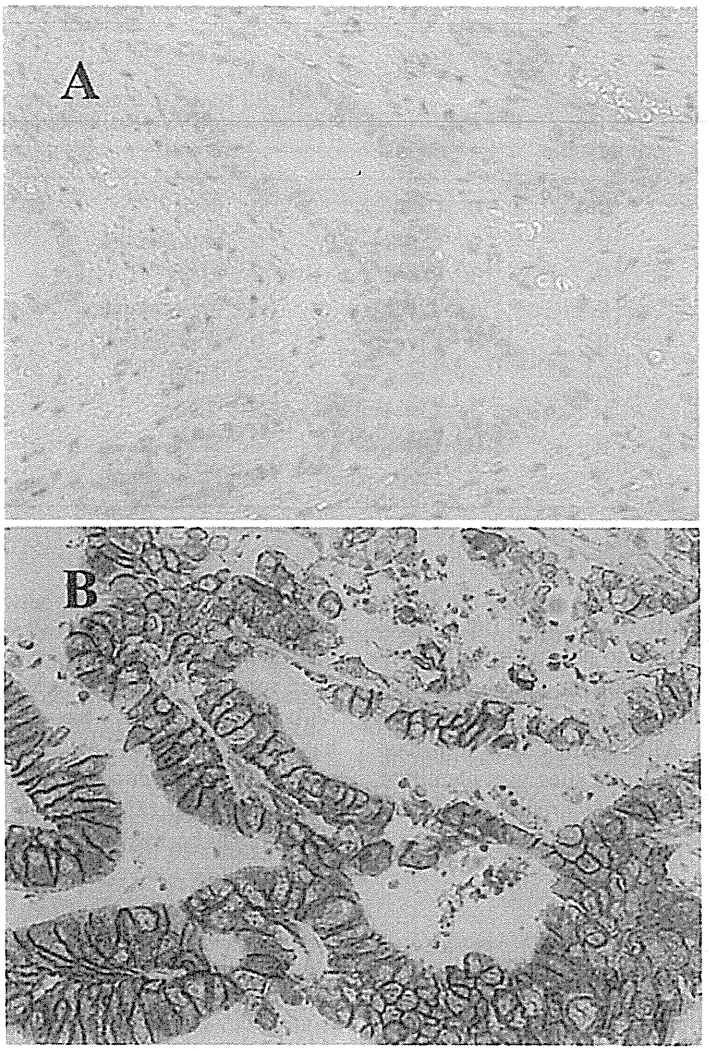

Figure 1. Human epidermal growth factor receptor 2 (HER2) expression by immunohistochemistry (A) at the primary site and (B) at paired metastatic sites. The histological type at the primary site was moderately differentiated tubular adenocarcinoma and HER2 status was scored as 0. The metastatic site was the liver and HER2 status was scored as 3+. Magnification, x40.

HER2-positive status was defined as IHC 3+, or HER2 2+ and FISH-positive (HER2/CEP17 ratio >2). HER2-negative status was defined as IHC 0, 1+, or 2+ and FISH-negative; the positive groups were considered suitable for trastuzumab combination therapy (6). All IHC 2+ tumors were further analyzed with FISH to determine the HER2 gene copy level. All the tissue samples from metastatic sites enabled the pathologist to confirm the lesions as being metastatic from gastric cancer.

Statistical methods. For the evaluation of the correlations of HER2 status between primary and paired metastatic lesion, the Fisher's exact probability test was employed. $P<0.05$ was considered to indicate a statistically significant difference.

Results

Clinicopathological characteristics. The clinicopathological characteristics of the patients in this study are summarized in Table I. The metastatic sites included the peritoneum (n=20), liver (n=10), lung (n=7), skin and subcutaneous tissue (n=5), colon (n=3) and others (n=4) (data not shown).

HER2 IHC. The results for HER2 IHC are shown in Table II. The HER2 status of the primary sites was scored as 0 in 30 specimens (81%), 1+ in 1 (3%), 2+ in 1 (3%) and 3+ in 5 (13%), while metastatic sites were scored as 0 in 29 specimens (78%), 1+ in 1 (3%), 2+ in 0 (0%) and 3+ in 7 (19%). The HER2 positivity (IHC 3+ or 2+ and FISH-positive) ratio of primary sites was ~16%. The association of the HER2 status of the primary site with histological type and type of intervention are shown in Table III. The HER2 positivity ratio of the differentiated type was significantly higher compared to that of the undifferentiated type. However, there was no significant association between the HER2 status of the primary site and the type of intervention. The total concordance ratio between primary sites and metastatic sites was ~97% (Table IV), reflecting a significant correlation ($P<0.0001$). Only one case exhibited positive conversion (Fig. 1A and B). This case evaluated HER2 status between primary and paired metastatic sites

Table V. Human epidermal growth factor receptor 2 (HER2) status with metachronous interventions.

Case	Histology	HER2 status of the primary site	HER2 status in metachronous interventions				
			1st	2nd	3rd	4th	5th
1	Differentiated	0	0: Colon	0: Skin	0: Skin	0: Kidney	0: Skin
2	Undifferentiated	0	0: Colon	0: Peritoneum			
3	Undifferentiated	0	0: Colon	0: Liver			
4	Differentiated	0	3+: Liver	3+: Peritoneum			
5	Undifferentiated	0	0: Liver	0: Peritoneum			
6	Differentiated	3+	3+: Lung	3+: Lung			
7	Differentiated	3+	3+: Cerebellum	3+: Lung			
8	Undifferentiated	0	0: Ovary	0: Skin			
9	Undifferentiated	0	0: Peritoneum	0: Peritoneum			

by resected specimen. Although in this case all the portions of the primary site were examined, no positive reaction was observed on the membrane in any of the specimens. The equivocal (2+) case exhibited amplification by FISH and was therefore classified as positive. Although one case of discordance between primary and metastatic sites was identified, there were no discordances among metachronous metastatic sites (Table V).

Discussion

Previous studies have estimated the HER2 positivity ratio to be 8.1-17.1% in gastric cancer (6,15,16). Recent studies reported that the HER2 positivity ratio is lower in patients with curatively resectable gastric cancer compared to that in unresectable patients (15,16). The present study estimated an HER2-positive ratio of ~16%, presumably because the study population comprised patients with curatively resected and unresected or recurrent gastric cancer. In this study, the differentiated type of tumor exhibited a significantly high HER2 positivity, as the consensus reported that the majority of positive cases were histologically of the intestinal type (17). However, Lee *et al* (18) reported a discordance of the HER2 IHC score between biopsies and gastrectomies; in this study, there was no difference between bioptic and resected specimens, although only a small series was analyzed.

The HER2 status in gastric cancer is commonly evaluated immunohistochemically, with a IHC 2+ status further analyzed by FISH, since previous studies demonstrated a high concordance ratio between IHC and FISH in gastric cancer (11,13,14,17,19,20) and the American Society of Clinical Oncology/College of American Pathologists guidelines recommend that FISH analysis be conducted for cases with an IHC 2+ lesion in breast cancer (21). In gastric cancer, combination chemotherapy with trastuzumab was adopted from 2010 onwards and sufficient scientific evidence regarding HER2 has not yet been accumulated. Therefore, references have been made to previous studies regarding HER2 in breast cancer. Since metastatic sites from gastric cancer patients are rarely resected or biopsied, evidence on the concordance of HER2 status by IHC between primary tumor and paired metastatic lesions other than lymph nodes has not generally been reported (17,22). In breast cancer, a high concordance ratio between primary and matched metastatic lymph nodes has been reported (7,8). However, in parenchymal metastases, the concordance ratio was found to be lower (9,10). Nakamura *et al* (23) reported that biopsy of the metastatic lesions may be useful for determining treatment strategies. We examined the tumor invasive front at the primary sites in resected specimens, as it was previously reported that HER2 staining exhibits no preferential distribution within the tumor, with negligible variation between the tumor mucosal surface and the invasive front (24) and the tumor invasive front is closely involved in the metastatic process. However, Fusco *et al* (25) reported that there is discordance in the HER2 status between the tumor invasive front and other lesions and gastric cancer is known to exhibit heterogeneous HER2 expression (14,18). Therefore we examined all the sites of the primary tumor in the discordant case to determine whether there was heterogeneity of HER2 expression, in order to assess the discordance between primary and paired metastatic lesions. However, all the lesions were IHC-scored as 0. In addition, we investigated whether there exists discordance among metachronous multiple interventions. A limited number of studies (17,22,26) have addressed such issues in gastric cancer. Kim *et al* (17) reported significant discordance (13.1%) between primary and metastatic lesions by IHC, but no discordance by FISH. Bozzetti *et al* (22) reported a concordance ratio of 94.9% between primary and matched metastatic lesions by IHC. In addition, Kochi *et al* (26) reported a discordance ratio of 9.8% in the HER2 status between primary sites and metastatic lymph nodes by FISH and IHC. Our results using IHC revealed a high concordance ratio (~97%) between primary and paired metastatic lesions. These results suggest the efficacy of HER2 status examination in the primary lesion for assessing the status of parenchymal metastatic lesions. Only one case of positive conversion was found in our study; likewise, Bozzetti *et al* (22) reported only a single case of discordance between the primary lesion and metastasis. The discordant case in this study was IHC 0 at the

primary site and underwent liver resection for metachronous liver recurrence following hepatic intra-arterial chemotherapy (fluorouracil + cisplatin + irinotecan). The HER2 status of the liver specimen at that time was IHC 3+ and the HER2 status of the metachronous peritoneal recurrent specimen was also IHC 3+. These findings suggest that the transition of the metastatic process strongly involves the discordance of HER2 status between primary and metastatic sites rather than heterogeneity of HER2 expression within the primary lesion. Further investigation of this issue in a larger series is required.

Nine patients underwent metachronous multiple interventions for metastatic lesions; no cases of discordance during the therapeutic period were encountered. To the best of our knowledge, no previous studies have reported such findings.

Unfortunately, no cases in this study population received trastuzumab combination therapy and further investigation, including those cases, is required.

In conclusion, the concordance ratio for HER2 status between primary and parenchymal metastatic or recurrent lesions was high. Therefore, determining the HER2 status in the primary lesion may be acceptable when considering the suitability of anti-HER2 agents for patients with inoperable advanced or recurrent gastric cancer.

Acknowledgements

The authors wish to thank Yuki Mutsumi for assisting with IHC and FISH.

References

1. Kamangar F, Dores GM and Anderson WF: Patterns of cancer incidence, mortality, and prevalence across five continents: defining priorities to reduce cancer disparities in different geographic regions of the world. J Clin Oncol 24: 2137-2150, 2006.
2. Parkin DM, Bray F, Ferlay J and Pisani P: Global cancer statistics, 2002. CA Cancer J Clin 55: 74-108, 2005.
3. Otsuji E, Yamaguchi T, Sawai K, *et al*: Recent advances in surgical treatment have improved the survival of patients with gastric carcinoma. Cancer 82: 1233-1237, 1998.
4. Horner MJ, Ries LAG, Krapcho M, *et al*: SEER Cancer Statistics Review, 1975-2006. http://seer.cancer.gov/archive/csr/1975_2006/results_merged/sect_24_stomach.pdf. Accessed April 12, 2009.
5. Cunningham SC, Kamangar F, Kim MP, *et al*: Survival after gastric adenocarcinoma serection: eighteen-year experience at a single institution. J Gastrointest Surg 9: 718-725, 2005.
6. Bang YJ, Van Cutsem E, Feyereislova A, *et al*: Trastuzumab in combination with chemotherapy versus chemotherapy alone for treatment of HER2-positive advanced gastric or gastro-oesophageal junction cancer (ToGA): a phase 3, open-label, randomized controlled trial. Lancet 376: 687-697, 2010.
7. Cardoso F, Di Leo A, Larsimont D, *et al*: Evaluation of HER2, p53, bcl-2, topoisomerase II-alpha, heat shock proteins 27 and 70 in primary breast cancer and metastatic ipsilateral axillary lymph nodes. Ann Oncol 12: 615-620, 2001.
8. Simon R, Nocito A, Huebscher T, *et al*: Patterns of her-2/neu amplification and overexpression in primary and metastatic breast cancer. J Natl Cancer Inst 93: 1141-1146, 2001.
9. Chang HJ, Han SW, Oh DY, *et al*: Discordant human epidermal growth factor receptor 2 and hormone receptor status in primary and metastatic breast cancer and response to trastuzumab. Jpn J Clin Oncol 41: 593-599, 2011.
10. Chan A, Morey A, Brown B, *et al*: A retrospective study investigating the rate of HER2 discordance between primary breast carcinoma and locoregional or metastatic disease. BMC Cancer 12: 555, 2012.
11. Marx AH, Tharun L, Muth J, *et al*: HER-2 amplification is highly homogenous in gastric cancer. Hum Pathol 40: 769-777, 2009.
12. Fassan M, Ludwig K, Pizzi M, *et al*: Human epithelial growth factor receptor 2 (HER2) status in primary and metastatic esophagogastric junction adenocarcinomas. Hum Pathol 43: 1206-1212, 2012.
13. Tafe LJ, Janjigian YY, Zaidinski M, *et al*: Human epidermal growth factor receptor 2 testing in gastroesophageal cancer: correlation between immunohistochemistry and fluorescence in situ hybridization. Arch Pathol Lab Med 135: 1460-1465, 2011.
14. Hofmann M, Stoss O, Shi D, *et al*: Assessment of a HER2 scoring system for gastric cancer: results from a validation study. Histopathology 52: 797-805, 2008.
15. Kunz PL, Mojtahed A, Fisher GA, *et al*: HER2 expression in gastric and gastroesophageal junction adenocarcinoma in a US population: clinicopathologic analysis with proposed approach to HER2 assessment. Appl Immunohistochem Mol Morphol 20: 13-24, 2012.
16. Kataoka Y, Okabe H, Yoshizawa A, *et al*: HER2 expression and its clinicopathological features in resectable gastric cancer. Gastric Cancer 16: 84-93, 2013.
17. Kim MA, Lee HJ, Yang HK, *et al*: Heterogeneous amplification of ERBB2 in primary lesions is responsible for the discordant ERBB2 status of primary and metastatic lesions in gastric carcinoma. Histopathology 59: 822-831, 2011.
18. Lee S, de Boer WB, Fermoyle S, *et al*: Human epidermal growth factor 2 testing in gastric carcinoma: issues related to heterogeneity in biopsies and resections. Histopathology 59: 832-840, 2011.
19. Takehara T, Kunitomo K, Kono K, *et al*: Status of c-erbB-2 in gastric adenocarcinoma: a comparative study of immunohistochemistry, fluorescence in situ hybridization and enzyme-linked immuno-sorbent assay. Int J Cancer 98: 833-837, 2002.
20. Yano T, Doi T, Ohtsu A, *et al*: Comparison of *HER2* gene amplification assessed by fluorescence *in situ* hybridization and HER2 protein expression assessed by immunohistochemistry in gastric cancer. Oncol Rep 15: 65-71, 2006.
21. Wolff AC, Hammond ME, Schwartz JN, *et al*; American Society of Clinical Oncology; College of American Pathologists: American Society of Clinical Oncology/College of American Pathologists guideline recommendations for human epidermal growth factor receptor 2 testing in breast cancer. J Clin Oncol 25: 118-145, 2007.
22. Bozzetti C, Negri FV, Lagrasta CA, *et al*: Comparison of HER2 status in primary and paired metastatic sites of gastric carcinoma. Br J Cancer 104: 1372-1376, 2011.
23. Nakamura R, Yamamoto N, Onai Y, *et al*: Importance of confirming HER2 overexpression of recurrence lesion in breast cancer patients. Breast Cancer 20: 336-341, 2013.
24. Kim KC, Koh YW, Chang HM, *et al*: Evaluation of HER2 protein expression in gastric carcinomas: comparative analysis of 1,414 cases of whole-tissue sections and 595 cases of tissue microarrays. Ann Surg Oncol 18: 2833-2840, 2011.
25. Fusco N, Rocco EG, Del Conte C, *et al*: HER2 in gastric cancer: a digital image analysis in pre-neoplastic, primary and metastatic lesions. Mod Pathol 26: 816-824, 2013.
26. Kochi M, Fujii M, Masuda S, *et al*: Differing deregulation of HER2 in primary gastric cancer and synchronous related metastatic lymph nodes. Diagn Pathol 8: 191, 2013.